https://doi.org/10.5194/egusphere-2025-1420
Preprint. Discussion started: 16 April 2025

Drone-based vertical profiling of particulate matter size distribution and carbonaceous aerosols: urban vs. rural environment

Kajal Julaha[1,2,*], Vladimír Ždímal[2], Saliou Mbengue[3], David Brus[4], Naděžda Zíková[2,5,*]

[1]Department of Atmospheric Physics, Faculty of Mathematics and Physics, Charles University, Prague, 18000, Czech Republic.
[2]Institute of Chemical Process Fundamentals of the Czech Academy of Sciences, Prague 16500, Czech Republic.
[3]Global Change Research Institute of the Czech Academy of Sciences, Brno 60300, Czech Republic.
[4]Atmospheric Composition Research, Finnish Meteorological Institute, Helsinki 00560, Finland.
[5]Institute for Environmental Studies, Faculty of Sciences, Charles University, Prague, 12801, Czech Republic

*Correspondence to: zikova@icpf.cas.cz (*N. Zíková*), julaha@icpf.cas.cz (*K. Julaha*)

Keywords: Equivalent black carbon, vertical distributions, Drone, micro-aethalometer AE51, optical particle counter, Aethalometer AE33, optical particle sizer, humidity control.

Abstract. The study uses drone-based measurements to investigate the seasonal vertical variability of equivalent black carbon (eBC) mass and particle number concentrations (PNC) at a rural and urban site in the Czech Republic. Vertical profiles of eBC were measured using a micro-aethalometer, while PNC was measured using an optical particle counter. Drone-based eBC measurements closely matched reference aethalometers placed at both ground level and at 230m of a tower when using a humidity control mechanism. Without dryer, eBC mass concentration was overestimated by 276% in summer and 285% in winter, but uncertainties were reduced to under 10% with drying. These findings highlight the importance of humidity control for accurate aerosol measurements, especially for eBC. The study also revealed a decrease in eBC and PNC with height at the rural site during both summer and winter, with seasonal differences in the altitude where this decrease began. Elevated eBC concentrations in winter were due to increased atmospheric stability and combustion-related fine particles. At the urban site, concentrations in summer were uniform with height (4 to 100 m AGL) but gradually decreased with height during winter. Furthermore, the study investigated changes in the vertical distribution of eBC and PNC during a high pollution event at the urban site, influenced by long-range transport. Our findings confirm the effectiveness of drones in capturing vertical variations of air pollutants, offering results on the dynamics between local emissions, atmospheric stability, and long-range transport and suggesting the necessity of vertical pollutants' concentration measurements to support air quality management strategies.

1. Introduction

Black Carbon (BC) aerosols, one of the substantial contributors to climate change and adverse health effects, are primarily emitted into our atmosphere through incomplete combustion of fossil fuels and biomass (Bond et al., 2013; Ramanathan and Carmichael, 2008). BC absorbs efficiently solar radiation and contributes to atmospheric warming (Moteki, 2023; Myhre et al., 2013). Aged BC can act as cloud condensation nuclei (CCN) and affect climate through its indirect effects by altering cloud properties and their formation processes (Wang et al., 2018b). The radiative properties of BC depend on its vertical profiles (Samset et al., 2013). For example, BC in the free troposphere can enhance its radiative forcing by trapping energy emitted from the lower cloud layers (Schwarz et al., 2006). The vertical distribution of BC also impacts the evolution of the planetary boundary layer (PBL). BC

https://doi.org/10.5194/egusphere-2025-1420
Preprint. Discussion started: 16 April 2025

in the upper PBL exhibits light absorption efficiency, heating the surrounding atmosphere and enhancing atmospheric stability, leading to extreme haze pollution events (Ding et al., 2016).

Modeling-based studies on BC vertical distribution are limited (Chen et al., 2022). Uncertainties in these models mainly arise from assumptions about the vertical distribution of BC aerosols, highlighting the need to measure the vertical distribution of BC on a regional scale, from areas influenced by direct emissions from the ground to those characterized by long-range transport (Ramana et al., 2010). These measurements can also help validate satellite observations and improve the representation of BC vertical profiles in climate models, leading to a more accurate assessment of BC radiative forcing (Li et al., 2013; Samset et al., 2013).

The BC vertical distribution can be measured by various platforms, such as meteorological balloons, towers, aircraft, and unmanned aerial vehicles (UAVs). Meteorological tethered balloons provide highly resolved data and detailed information close to the ground, capable of measuring aerosol concentrations up to the free atmosphere (Babu et al., 2011; Ferrero et al., 2019; Renard et al., 2020; Cappelletti et al., 2022). Meteorological towers offer a unique opportunity for continuous long-term monitoring of aerosols at different heights (Chi et al., 2013; Xie et al., 2019; Sun et al., 2020; Liang et al., 2022). Compared to towers, aircraft and UAVs can access higher altitudes, with some aircraft capable of carrying heavier payloads, allowing them to transport more sophisticated instruments for detailed aerosol measurements. These platforms offer greater spatial coverage and flexibility, making them suitable for comprehensive atmospheric studies (Brady et al., 2016; Corrigan et al., 2007; Villa et al., 2016; Wu et al., 2021; Schulz et al., 2019). Drones have recently gained popularity among all the other methods because of their cost effectiveness, flexibility, and mobility due to their lightweight design (Barbieri et al., 2019; Boer et al., 2020). Several studies have used drones to study vertical measurements of BC and particle number concentrations (PNC). For example, Liu et al. (2020) conducted vertical measurements of fine particulate matter (PM) and BC using a DJI Matrice 600 drone equipped with a battery-operated light-scattering laser photometer and a micro-aethalometer. Their study revealed different vertical patterns for PM2.5 and BC, suggesting different sources for each. Similarly, Zhu et al. (2019) used a hexacopter with a customized scanning mobility particle sizer, an optical particle counter, and a meteorology sensor to study the vertical variability of particle number size distribution (PNSD) near the ground to up to 300 m. The study showed that PNC with size >0.3 μm decreased with height during the evening. Brus et al. (2021) investigated the vertical profile of PNCs and gases in the San Luis Valley, Colorado, and highlighted their interaction with meteorological conditions and boundary layer processes. Studies on the vertical distribution of BC aerosols in Central Europe are very limited. In Poland, Chilinski et al. (2016) examined the vertical distribution of BC in a valley for three days using UAV. In Germany, Samad et al. (2020) investigated the vertical profiles of PM, BC, and ultrafine particles in Stuttgart using a tethered balloon, and Harm-Altstädter et al. (2024) used a fixed-wing drone for vertical measurement of aerosol concentration, including eBC, near a civil airport.

The studies about the vertical distributions of BC aerosols in the Czech Republic are limited to a tall tower in a rural area (Mbengue et al., 2023), and no measurements in urban areas have been done. To date, no drone-based measurement of BC has been conducted in the Czech Republic. This study combines mobile (drone-based) and fixed (tall tower and building) observational platforms to measure the vertical distribution of BC aerosols and PNC at two different sites representing an urban and a rural location. It further estimates the measurement uncertainties and dependence of the results on the humidity.

https://doi.org/10.5194/egusphere-2025-1420
Preprint. Discussion started: 16 April 2025

2. Materials and Methodology

2.1. Measurement Sites

2.1.1. Rural background site

The National Atmospheric Observatory Košetice (NAOK, 49°35′N, 15°05′E; 534 m a.s.l.) in the Bohemian Moravian Highlands in the Czech Republic (Figure 1) represents a central European background site. Located approximately 75 kilometers southeast of Prague, the observatory is situated in a rural area. The observatory is equipped with instruments to measure gaseous pollutants, atmospheric aerosols, and meteorological parameters. It also includes a 250 m tall atmospheric tower providing a unique opportunity to study atmospheric parameters at different elevations (Dvorská et al., 2015). NAOK is part of the Aerosol, Clouds, and Trace Gases Research Infrastructure Network (ACTRIS ERIC) and several other research projects and monitoring programs (Mbengue et al., 2023).

NAOK is influenced by regional and long-range transported air masses, mainly associated with the western and southeastern directions (Mbengue et al., 2021; Vodička et al., 2015). A primary highway in the Czech Republic (D1: 36,000 cars/day, CSD, 2020) is situated approximately 6 km to the north and northeast of the observatory (Mbengue et al., 2023).

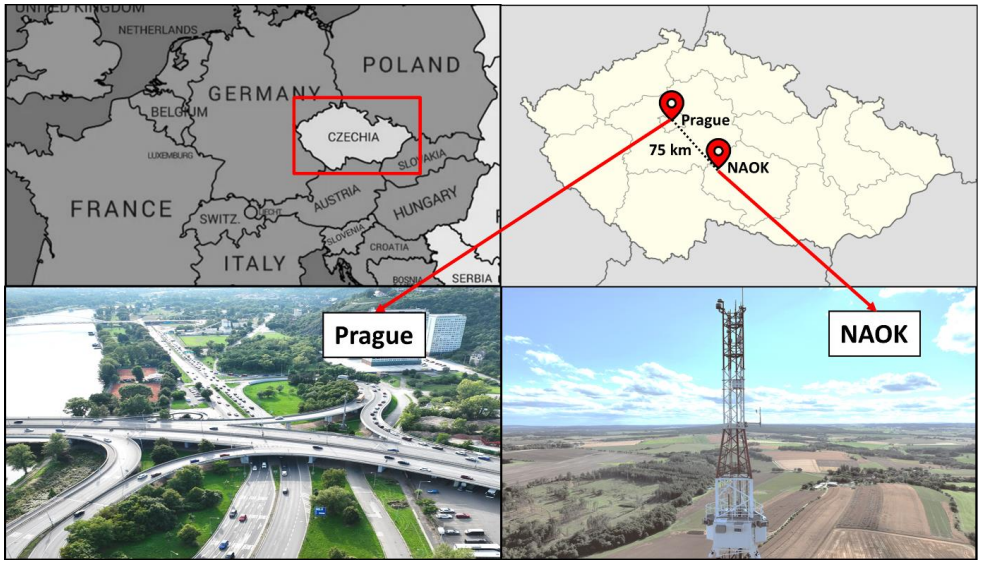

Figure 1. Geographical location of rural background (NAOK) and urban (Prague) sites in the Czech Republic. Source: mapchart.net, Wikipedia.

2.1.2. Urban site

The Faculty of Mathematics and Physics (50°6.89′N, 14°26.95′E; 185 m a.s.l.) at Charles University in Prague represents an urban site situated 75 kilometers away from NAOK (Figure 1). The faculty has multiple campus locations throughout Prague, with its Troja campus near the Vltava River serving as the site for this study. The

https://doi.org/10.5194/egusphere-2025-1420
Preprint. Discussion started: 16 April 2025

main building of the Troja campus is an 11-story building, almost 50 m high. The campus is located in a river valley surrounded by hills with an elevation of 50 m AGL. The Department of Atmospheric Physics (DAP) is also on this campus. The DAP monitors particulate matter (PM_1, $PM_{2.5}$, and PM_{10}), gases (NO_2, O_3, and CO), and meteorology (temperature, relative humidity (RH), pressure, wind speed, and rainfall), with measurements taken at ground level (2m), 10 m, and 50 m (Ramatheerthan et al., 2024).

The site is located near the Blanka tunnel exit and is impacted by fresh traffic emissions. The Blanka tunnel, more than 6 km long, is the longest road tunnel in the Czech Republic. The average traffic density of this tunnel is 80,000 to 90,000 cars/day (Metrostav, 2024). It was constructed to minimize the environmental impacts of traffic. However, its opening significantly increased the traffic at some locations, leading to substantial changes in the urban geochemistry of Prague (Mizera et al., 2022).

2.2. Instrumentation

2.2.1. eBC measurements

The micro-Aethalometer AE51 (AethLabs San Francisco, CA) (Figure 2a) provides real-time equivalent BC (eBC) concentration using an 880 nm light source (Petzold et al., 2005). AE51 operates on a principle similar to other aethalometers, such as AE31 (Aerosol Magee Scientific, Berkeley, CA). The AE51 measures the light attenuation through a filter (T60 Teflon-coated glass fiber) loaded with particles and converts the attenuation into an eBC mass concentration using a predefined mass attenuation coefficient (Alas et al., 2020). The time resolution of 10 seconds and flow rate of 150 ml/min were used in this study. The filter was replaced when attenuation reached 80 dB/m to minimize the filter loading effect.

2.2.2. Air stream Dryer

A 20 cm-long homemade silica gel dryer (Figure 2d) was used in front of the AE51 (Figure 2f) to control the humidity for accurate eBC mass concentrations measurements. The dryer consists of 2 coaxial cylinders of 1.62 cm and 0.65 cm diameters, with silica gel in the space between them. The silica gel effectively removes moisture from the aerosols as axial airflow passes through the dryer. The inner cylinder, made from stainless steel mesh, was chosen for its smooth surface and minimal particle loss, while the outer parts were fabricated with PLA (Polylactic Acid) using a 3D printer (MK4S, Prusa Research), with a total weight of 50 g. Laboratory tests were performed at 100% RH, showing that the dryer could perform effectively by maintaining RH below 40% for up to three days (Figure S1). The flow and leakage tests were also carried out to describe the dryer's performance.

2.2.3. Particle number concentration measurements

The air quality measurements backpack (Yugen Oy, Finland) for a consumer-grade drone with an Optical particle Counter (OPC-N3, Alphasense) (Figure 2b) was used to measure PNC in the PSL equivalent size range from 0.35 to 40 µm. The OPC detects the light scattered by particles in the sample air stream illuminated by a laser beam (~658 nm) and translates the signal into particle count and size (Hagan and Kroll, 2020). The backpack uses a Raspberry Pi zero microcomputer as a data logger and was mounted on the top of the drone (Figure 2g). The backpack also contains two meteorological sensors BME 280 (Bosch Sensortec GmbH) and SHT85 (Senserion AG) positioned on either side of the backpack and a redundant to drone own GPS module for the recording of

https://doi.org/10.5194/egusphere-2025-1420
Preprint. Discussion started: 16 April 2025

drone position (Brus et al., 2025). Temperature and RH readings from both sensors were compared against tower-based temperature and RH data while flying on the drone at different heights to validate sensor accuracy and data reliability (Figure S2-S5). Both the BME280 and SHT85 sensors exhibit correlations about or over 0.9 between tower measurements and temperature across various heights. However, at 230 m, this correlation weakens to 0.5. For humidity, the SHT85 maintains a strong correlation at most heights, except at 230 m, while the BME280 shows greater variability, with R^2 values dropping to 0.54 at 4 m, 50 m, and 230 m. Due to OPC's horizontal inlet design and a built-in ventilator, equipping a dryer was not feasible, as it would result in an excessively high pressure drop making the measurement highly unreliable.

The total particle number concentration (N), in particles per cubic meter (#/m^3), was calculated from the raw OPC data as:

$$N = \frac{C}{F \cdot t}, \quad (1)$$

where C is the total particle count, F is the flow rate in cm^3/s, and t is the sampling time in seconds. The OPC operates at a total flow rate of 5.5 l/min and a sample flow rate of 0.21 l/min. The measurement interval of 1 second was used to account for the high temporal variability of particles' concentrations.

2.2.4. Temperature and RH

For OPC, sensor SHT85 was used to measure ambient temperature (T) and RH, while with AE51, an Arduino (MKR Zero) datalogger (HYT939p, Innovative Sensor Technology IST AG) (Figure 2c) was used for T and RH measurements. The Arduino MKR zero microcontroller processes sensor data using a 32-bit SAMD21 processor and stores it on an SD card. It is programmed via the Arduino IDE to read inputs, perform tasks, and save data. The Arduino datalogger with HYT939p sensor was developed after the first summer campaigns at both sites and, therefore, was used only during winter campaigns. For the summer campaign, meteorological variables from the tower at the same height as the drone hover at NAOK were used, and in Prague, meteorological data from the ground and top of the building, i.e., 50 m, were used. The Arduino T and RH measurements were also compared to the tower temperature and RH data at different heights to confirm the validity and robustness of the drone T and RH results (Figures S6 and S7). The results show a strong correlation between tower measurements and Arduino observed humidity and temperature at different heights, with R^2 values generally above 0.8.

https://doi.org/10.5194/egusphere-2025-1420
Preprint. Discussion started: 16 April 2025

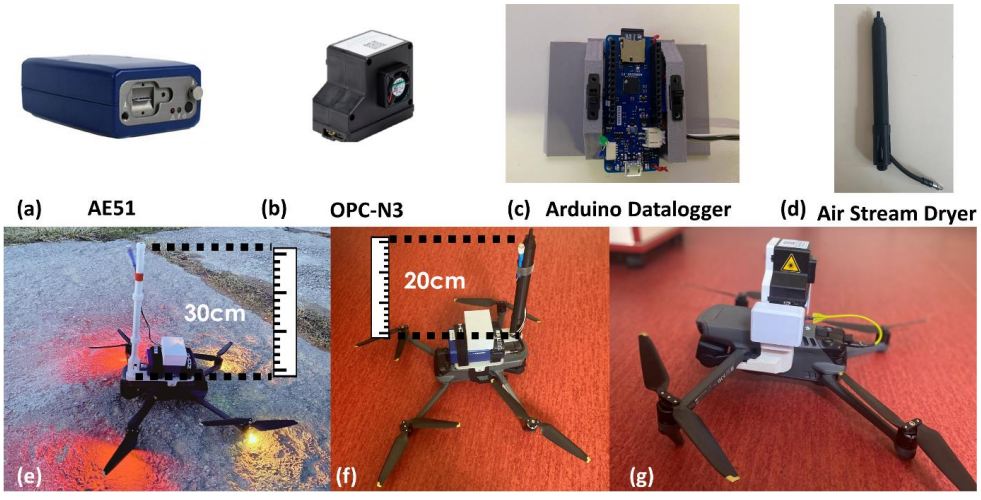

Figure 2. Measurement setup: (a) micro-Aethalometer AE51, (b) optical particle counter (OPC) N3, (c) Arduino datalogger, (d) Air Stream Dryer, (e) micro-Aethalometer AE51 with a temperature and RH datalogger without a dryer, (f) micro-Aethalometer AE51 with a temperature and RH datalogger with a dryer, and (g) consumer drone backpack with an optical particle counter with a custom mount on the drone.

2.2.5. Drone-based sampling

The instruments were installed on the Mavic 3 Classic drone (DJI Techology Co., Ltd.) (https://www.dji.com/cz/mavic-3-classic/specs). The instrument's combined weight was too high to be carried by the drone; thus, the instruments were set up separately and measured each alternating hour. With micro-Aethalometer AE51, two different types of inlets were used: a 30 cm high inlet without a dryer and a 20 cm high inlet with a diffusion-based silica gel dryer, while no inlet was used with a drone backpack (Figure 2). The particle loss within the inlet for particles up to 2.5 µm calculated for the AE51 setup for a 30 cm high inlet is ≤ 9%, and for a 20 cm dryer inlet, it is ≤ 1%. The overall sampling losses for the whole set-up were calculated using Particle Loss Calculator (von der Weiden et al., 2009) for all measurement set-ups and wind speeds (Table S1).

Only sampling losses were calculated for OPC and OPS, as no inlet extension was used. For OPS, sampling loss was minimal (10 % overestimation) for $PM_{2.5}$ fraction up to wind speed of 6 m/s, but PM_{10} showed an underestimation of 100 % up to 6 m/s. For OPC, sampling losses were less severe (50 % overestimation up to 6 m/s) for PM_1, but for $PM_{2.5}$, overestimation ranged from 60 % to 125 % at 4 m/s and 6 m/s, respectively. For PM_{10} particles, overestimation was as high as 750% at 6 m/s.

Whole inlet particle losses were calculated for AE51 with and without dryer inlets. For AE51 without a dryer, changes in concentrations for $PM_{2.5}$ remained minimal (< 10% overestimation) up to 4 m/s and below but increased at higher wind speeds, reaching up to 22 % overestimation for PM_1 at 6 m/s. For AE51 with dryer, sampling is also affected by wind speed, with overestimation increasing from 5 % at 2 m/s for PM_1 to 50 % at 6 m/s for $PM_{2.5}$.

https://doi.org/10.5194/egusphere-2025-1420
Preprint. Discussion started: 16 April 2025

During the flights, the drone climbed vertically from the ground to 230 m and 100 m AGL at a constant speed of 1 ms^{-1} along the tower at NAOK and the Prague building, respectively (the maximum altitude was limited to 100 m in Prague due to flight height restrictions). The drone hovered at different heights (4 m, 50 m, 100 m, 150 m, and 230 m at NAOK and 4 m, 50 m, and 100 m in Prague) for at least 3-5 minutes and then ascended in the same vertical direction. The descended flights were not considered due to the propellers' effect on aerosols' flow. Flights were conducted for at least 4 to 5 days during a week, depending on the weather conditions.

The summer campaign took place at NAOK from July and August 2023, and the winter campaign in February 2024 (Table 1). Additionally, a test to evaluate the dryer's performance was conducted on August 13, 2024. In Prague, measurements were performed during two summer campaigns and one winter campaign across 2023 and 2024. The urban measurements were taken without a dryer in August 2023, and in December 2023, while a dryer was used for eBC measurements in June 2024 (Table 1). Measurements for each campaign began at 8 AM and continued until 8 PM in summer and until 5 PM during winter due to shorter daylight hours. The number of flights for eBC and PNC at each height is summarized in Table 1.

Table 1. Overview of campaign schedule and total number of flights for eBC and PNC measurements. Campaigns with a dryer are indicated with an asterisk.

	Season	Campaign Dates	Number of flights (eBC)	Number of flights (PNC)	Measurement height (m AGL)
NAOK	Summer	July 31 to August 4, 2023	20	18	4,50,100,150,230
	Summer*	August 13, 2024*	12*	---	4*,230*
	Winter	February 12 to 16, 2024	15	15	4,50,100,150,230
Prague	Summer	August 14 to 20, 2023	22	21	4,50,100
	Summer*	June 18 to 23, 2024*	21*	21*	4*,50*,100*
	Winter	December 12 to 18, 2023	17	17	4,50,100

2.2.6. Additional variables

At NAOK, two aethalometers AE33 were available as reference instruments: one at the ground with a PM_{10} sampling inlet (Leckel GmbH) at 4 m AGL and the other installed at the top of the tower, i.e., at 230 m with the same sampling head as on the ground. The data from these aethalometers were compared with the drone-based measurements while the drone hovered at corresponding heights. The AE33 at the ground uses a Nafion dryer (custom-made, TROPOS, Leipzig, Germany) to remove moisture from the sample stream, whereas AE33 at 230 m was connected to a Nafion dryer but was not supplied with dry air during the summer of 2023 and winter campaigns. An Optical Particle Sizer (OPS) (model 3330, TSI Inc., USA), without any dryer to ensure similar measurement conditions, was placed at 4 m for comparison with the measurement from OPC on the drone. In addition, temperature, RH, global radiation, wind speed and direction, and gaseous concentrations were obtained from standard measurements at multiple tower heights (50 m, 125 m, and 240 m) and ground level (4 m) (Dvorská et al., 2015), and ceilometer CL51 (Vaisala, Finland) was used for every hour boundary layer information (Julaha et al., 2025). The percentage difference (PD) was calculated to evaluate variability across measurements for comparing data across different heights and conditions:

https://doi.org/10.5194/egusphere-2025-1420
Preprint. Discussion started: 16 April 2025

$$PD = \frac{X_{ref} - X_{drone}}{X_{ref}} * 100, \quad (2)$$

where X_{ref} is concentration from reference device and X_{drone} is concentration from device on drone. The same approach was taken also for calculating the difference between heights.

The wind shear between the heights was calculated as the difference in wind speed (ΔWS) divided by the difference in altitude (Δz):

$$Wind\ Shear = \frac{\Delta WS}{\Delta z}, \quad (3)$$

given in m/s per 100 m.

Table 2. Variables and instrumentation used in this study.

	Instruments	variables	Measurement heights (m AGL)	
			NAOK	Prague
Drone	AethLabs AE51	eBC	4, 50, 100, 150, 230	4, 50, 100
	Alphasense OPC N3	PNC	4, 50, 100, 150, 230	4, 50, 100
	BME and SHT85	T, RH, P	4, 50, 100, 150, 230	4, 50, 100
	Arduino HYT939p	T, RH	4, 50, 100, 150, 230	4, 50, 100
	Drone (DJI Mavic 3 Classic)	ws	4, 50, 100, 150, 230	4, 50, 100
Fixed	Magee AE33	eBC	4, 230	-
	TSI OPS 3330	PNC	4	-
	Vaisala Ceilometer CL51	BLH/MLH	ground	-
	Tower measurements	T, RH, P, ws, wd	4, 50, 125, 240	-
	ENVISENS M-22-017	Global Radiation	ground	50
	Envitech ED-19-004, ED-19-005	PM	-	10, 50
	Aeroqual AQS1, Envitech M-22-016, M-22-017	NO2, O3, CO	-	2, 50
	Davis Vantage Pro2, Meteopress MD1017, MD1016	T, H, P, ws	-	10, 50
	ERA5	BLH	-	-

In Prague, long-term measurements alongside the building include data on temperature, RH, wind speed, gaseous concentrations, and particulate matter concentrations, monitored at ground level, 10 m, and at the top of a 50m high building (Table 2) (Ramatheerthan et al., 2024). Since ground-based measurements for the boundary layer were not available at the site, boundary layer height predictions were obtained from ERA5, a fifth-generation ECMWF (European Centre for Medium Weather Forecasting) reanalysis model produced by the Copernicus Climate Change Service (C3S). The hourly boundary layer height was obtained for the duration of campaigns (Hersbach et al., 2023).

https://doi.org/10.5194/egusphere-2025-1420
Preprint. Discussion started: 16 April 2025

3. Results and Discussion

3.1. Intercomparison and effect of RH on eBC and PNC measurements

The eBC and PNC measured while hovering the drone were compared with the observations from the reference devices from the NAOK tower at 4m and 230m for both the summer and winter campaigns. The AE51 on the drone overestimated the median reference eBC mass concentration by approximately 276 % at 4m and by 99 % at 230m during summer, with absolute differences of 0.32 µg/m^3 and 0.15 µg/m^3, respectively. The smaller overestimation at the top of the tower can be due to similar measurement conditions as both AE33 at 230 m and the AE51 on the drone were operating without any dryer (except Nafion without dry air in front of the AE33, which may have partially influenced the moisture content of the sampled air). The higher difference at 4m during the summer is likely due to high RH affecting the eBC measurements; while a Nafion dryer was installed in front of the AE33 on the ground, the AE51 on the drone without a dryer was strongly influenced. This was further confirmed when the RH dropped below 40 % on one day, and eBC mass concentrations from AE51 on the drone were comparable at both 4m and 230m with the reference devices (Figure S8).

During the winter campaign, median drone-based measurements using AE51 overestimated eBC mass concentrations by 285 % (0.7 µg/m^3) at 4 m and by 150 % (0.4 µg/m^3) at 230 m compared to the reference AE33 observations (Figure 3). This can be attributed again to the influence of humidity—at 4m, the AE33 was operated with a dryer, and the temperature gradient between inside the measurement container and the external environment at 230 m likely contributed to some drying effects as the sample travelled from the colder outdoor to the warmer indoor environment.

The PNC from OPC on the drone also showed overestimation compared to the OPS reference observations by 75 % (8 #/cm^3) and 129 % (30 #/cm^3) during summer and winter, respectively. The comparison was made using the same size bins, with the first bin of the OPC skipped and interpolation applied to align the bins between the two instruments. Both the OPC and OPS measurements were conducted without a dryer for both seasons, thus measuring aerosol PNC at ambient RH. The observed difference can be attributed to different sampling orientations: OPC inlet sampled horizontally against the wind, while OPS had a vertical inlet, causing different influence on sampling in both instruments. For OPS, the sampling showed overestimation within 10 % for $PM_{2.5}$ up to wind speed of 6 m/s. In contrast, for OPC, overestimation jumped to 60 % and 125 % for $PM_{2.5}$ at wind speeds of 4m/s and 6m/s, respectively. As a result, OPC tends to report higher particle concentration than the OPS, which contributes to the discrepancies observed in the PNC values.

https://doi.org/10.5194/egusphere-2025-1420
Preprint. Discussion started: 16 April 2025

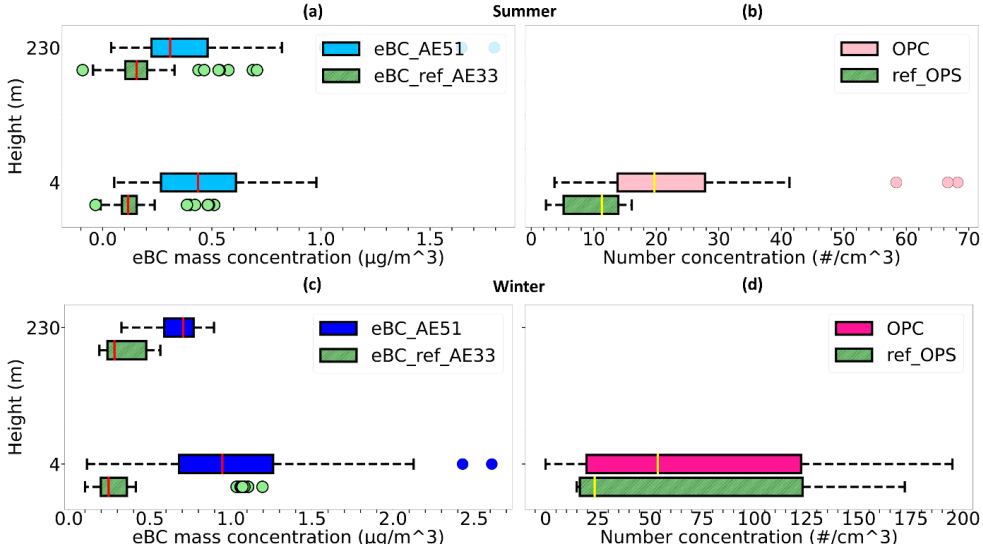

Figure 3. Boxplots of (a) eBC mass concentration and (b) PNC from drone vs. reference devices from the tower at 4 m and 230 m during the summer campaign at NAOK; c) and d) the same for winter.

To address the effect of RH on eBC concentrations from drone measurements, a homemade silica gel dryer was installed on the drone. A test to evaluate the dryer's performance was conducted on August 13, 2024, a typical summer day with a temperature of 28 °C, RH varying from 50% to 90%, and wind speed of 2-3 m/s. Additionally, the aethalometer on the top of the tower at NAOK was equipped with a nafion dryer to ensure consistent comparison between the two AE33 at different levels and between AE33 and AE51 under varying RH levels throughout the day. The eBC measurements were done with and without the dryer at the drone and compared to the AE33 eBC concentrations at the tower (both with Nafion dryers).

During this particular summer day, the AE51 on the drone without the dryer overestimated eBC mass concentrations by 29 % (0.09 µg/m^3) at 4 m and by 53 % (0.22 µg/m^3) at 230 m compared to the reference AE33 (Figure 4a). After installing the silica gel dryer on the drone, the eBC measurements were closely aligned with the reference observations, with the difference reduced to under 10% (0.01 µg/m^3 at 4 m and 0.02 µg/m^3 at 230 m) at both heights (Figure 4b). This highlights the significant role of the dryer in minimizing the humidity impacts and enhancing the accuracy of eBC mass concentration measurements from the micro-aethalometer AE51. These findings further confirm the reliability of the drone platform and its effectiveness in providing eBC measurements that compare well with long-term tower observations.

https://doi.org/10.5194/egusphere-2025-1420
Preprint. Discussion started: 16 April 2025

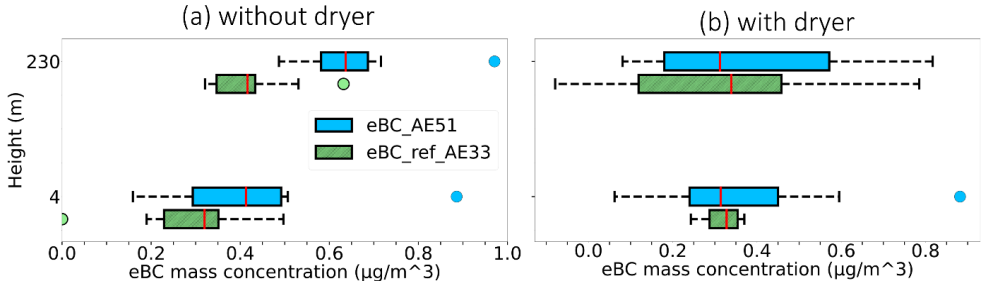

Figure 4. Boxplots of eBC mass concentration from drone and reference devices on the tower at NAOK during a summer day (August 13, 2024) at 4 m and 230 m (a) without the dryer and (b) with the dryer.

3.2. Aerosol vertical profile at the rural site

Vertical profiles of eBC mass concentrations without the silica gel dryer and PNC were measured while hovering the drone at different heights (4 m, 50 m, 100 m, 150 m, and 230 m) during the summer 2023 and winter 2024 at NAOK simultaneously with the reference instruments (Figure 5). During summer, eBC mass concentration remained relatively uniform up to the height of 50 m, followed by a decrease of 32 % (0.13 µg/m^3) between 50 and 100m. Conversely, PNC dropped by 30 % (6 #/cm^3) between 4 m and 50 m. In winter, eBC mass concentration stayed constant up to 100 m and decreased by 18 % (0.16 µg/m^3) between 100 m and 150 m. PNCs were constant from the ground to 50 m but decreased by 39 % (24 #/cm^3) between 50 m and 100 m. The significance of the increase or decrease in eBC mass concentration and PNC was tested by the Kruskal-Wallis (KW) test ($p < 0.05$).

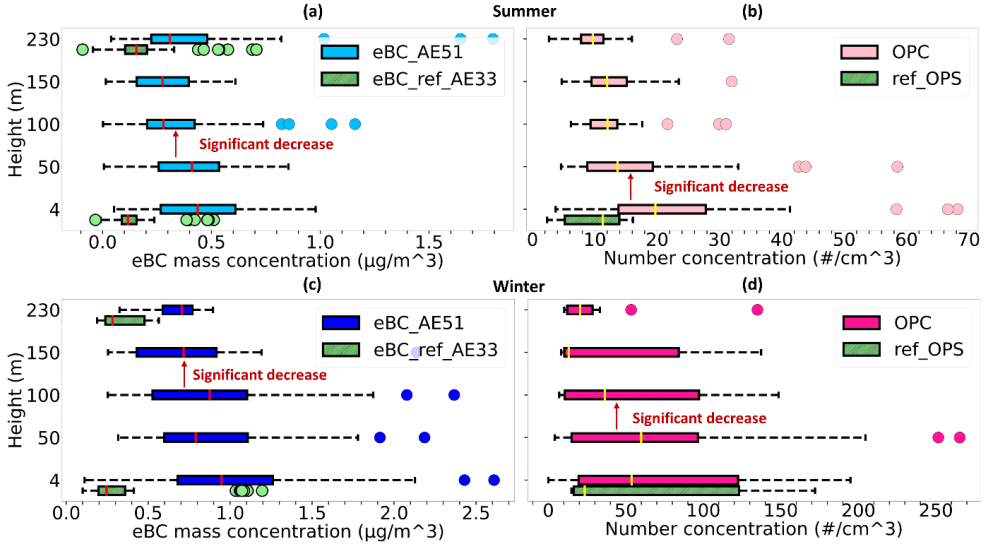

Figure 5. Boxplots of (a) eBC mass concentration and (b) PNC from the drone while hovering at different altitudes during summer at NAOK; c) eBC mass concentration and (d) PNC from the drone while hovering at different altitudes during winter at NAOK.

https://doi.org/10.5194/egusphere-2025-1420
Preprint. Discussion started: 16 April 2025

Simultaneously, the vertical gradient of temperature and RH were examined during the winter campaign to explain the vertical changes in eBC and PNC. The eBC, PNC, temperature, and RH comparison revealed no significant temperature variation from the ground to 50m for both eBC mass and PNC (Figure 6). The uniform temperature suggests stable atmospheric conditions that likely contributed to the accumulation of eBC and PNC within the first 50 m. Previous studies reported such patterns, where primary emissions near the surface get trapped under stable atmospheric conditions, leading to elevated concentrations of pollutants near the ground (Altstädter et al., 2020). The temperature started to decrease with height above 50 m, and the PNCs decreased, while eBC mass concentrations remained constant up to 100 m despite the temperature changes. This vertical pattern is similar to the summer measurements, where eBC mass was uniform up to 50 m, and PNC decreased from the ground. This indicates that differences in particle size may have brought the observed changes in PNC compared to the unaffected eBC mass concentrations.

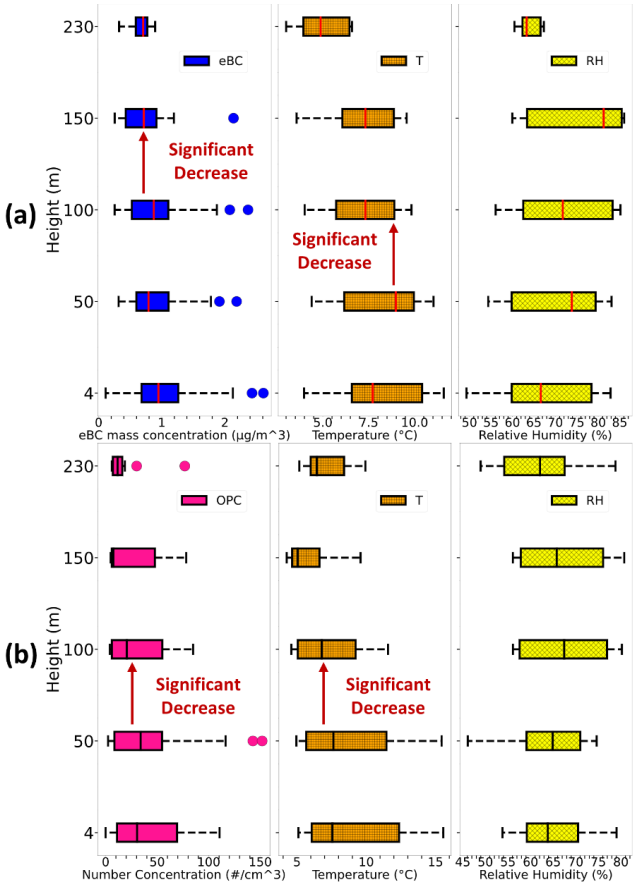

Figure 6. Boxplots of (a) vertical distribution of eBC mass concentration from AE51 without dryer, temperature, and RH, and (b) vertical distribution of PNC from OPC, temperature, and RH on the drone at NAOK from February 12 to 16, 2024.

https://doi.org/10.5194/egusphere-2025-1420
Preprint. Discussion started: 16 April 2025

Further, the decrease in eBC mass concentration with height was more pronounced in summer (32 %) compared to winter (18 %) at NAOK. On the contrary, PNC decreased with height more during winter (39 %) than in summer (30 %). While vertical mixing influences the vertical distribution of particles, the behavior of eBC vertical distributions reflects the combination of particle size and atmospheric stability rather than primarily depending on vertical mixing alone (Wang et al., 2018). Our results suggest that at least two aerosol populations of different sizes and sources were measured during the year, thus with different vertical behaviors.

3.3. Aerosol vertical profiles at the urban site

At the urban site, eBC mass concentration and PNC measurements were conducted up to 100 m during summer in two different years – 2023 and 2024. The eBC mass concentrations were measured without the dryer from August 14 to August 20, 2023, and with the dryer from June 18 to June 23, 2024. During both summers, eBC mass concentration and PNC were uniform up to the height of 100m (Figure 7). This consistency can be attributed to several factors. The high number of traffic emission sources at the site contributes to high and relatively stable eBC concentrations in the lower atmosphere, similar to the results of (Liu et al., 2023). Also, enhanced thermal convection and the urban heat island effect facilitate effective vertical mixing (Battaglia et al., 2017). Furthermore, wind shear above 20 m/s per 100 m between all the heights (4-50m and 50-100m) during both years supports the vertical transport of pollutants. The deeper and thermally driven convective boundary layer during summer further increased turbulence, and vertical mixing helped to distribute the particles more evenly within the lower atmospheric layers, thereby homogenizing the particle concentrations.

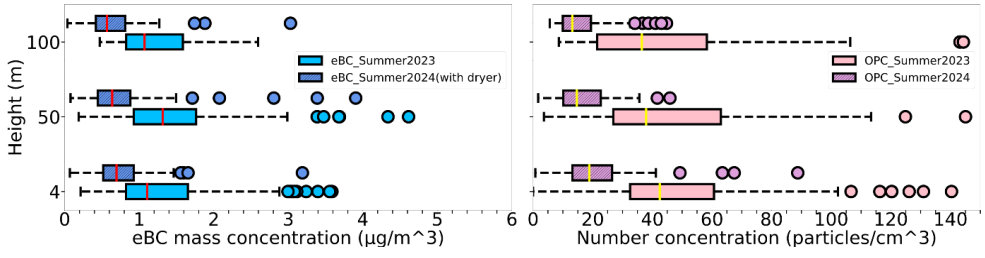

Figure 7. Boxplots of eBC concentration from AE51 without a dryer (summer 2023) vs. with a dryer (summer 2024) (left) and PNC from OPC at Prague during summer 2023 and 2024 (right).

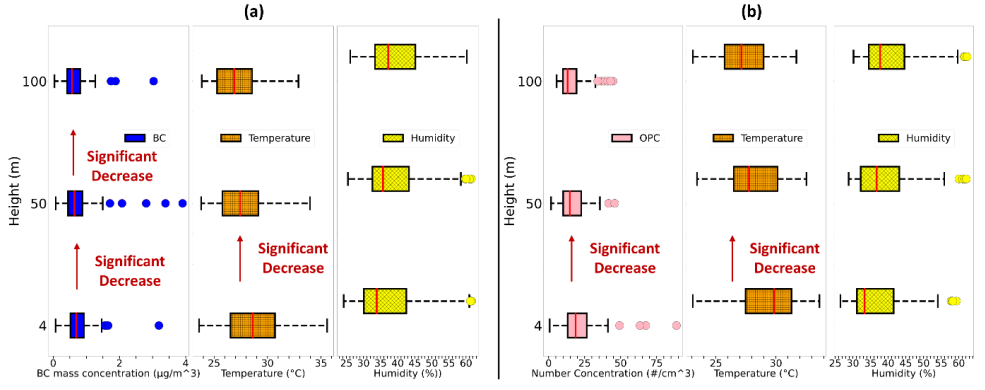

https://doi.org/10.5194/egusphere-2025-1420
Preprint. Discussion started: 16 April 2025

Figure 8. Boxplots of (a) eBC mass concentration from AE51 without dryer vs. Temperature vs. RH, and (b) PNC from OPC vs. Temperature vs. RH on the drone at Prague from December 12 to December 18, 2023.

During the winter campaign at Prague from December 12 to December 18, 2023, a significant reduction in both eBC mass concentration and PNC with increasing altitude was observed (Figure 8), contrasting with the summer pattern. Specifically, eBC mass concentration decreased with height up to 100 m, while PNC dropped to 50 m from the ground and remained constant between 50 and 100 m. This behavior is mainly influenced by the combination of strong emission sources in the urban environments, as described previously, and typical stable atmospheric conditions in winter, preventing vertical mixing. The relatively smaller wind shear (11 m/s per 100 m between 50 – 100 m) further suppresses vertical mixing, trapping pollutants near the surface (Figure S9). As a result, pollution remains confined closer to the emission sources, leading to higher concentrations near the ground and a more pronounced decrease with height (Kotthaus et al., 2023). Additionally, the urban heat island effect intensifies during stable conditions, causing temperature contrast between urban and rural areas, further reducing the vertical dispersion of pollutants (Haeffelin et al., 2024).

Several outliers (extremely high levels) were detected in the eBC mass and PNC. During summer, the outliers can be linked to increased turbulences and convective activities typically present during the warmer months, which lead to more variability in pollutant dispersion (Lumet et al., 2024). Fewer outliers were observed at NAOK for eBC and PNC during winter, but more pronounced outliers were present in winter measurements at Prague. This high concentration was due to a high pollution event between December 13 and 14, 2023. This event was marked by a sharp rise in PM levels, as confirmed by low visibility signals from the drone at 100 m and ongoing PM measurements at the site (Figure S10). The vertical variation and other characteristics of this pollution episode were thus further studied to get a better understanding of the influence of such an event on air quality.

3.4. Vertical variation during a high pollution event in Prague

An increase in eBC mass concentration and PNC characterized Prague's pollution event in December 2023. The event started on December 13th at 13:00 and lasted until the morning of December 14th, 2023. This concentration increase was primarily attributed to a low and stable boundary layer reaching 105 m above the ground (Figure S11). The vertical variation of eBC and PNC, along with the size distribution, was assessed to evaluate the changes one day before (i.e. December 12) and comprised 5 vertical profiles of eBC and 4 profiles of PNC. During the event, 3 profiles for both eBC and PNC were measured, all showing a substantial increase in concentrations at all heights (4m, 50m, and 100m) compared to the period before the pollution episode (Figure S12).

The highest increase in eBC concentrations during the event was observed at 100 m, with a 192% (2.5 $\mu g/m^3$) increase in median eBC levels compared to that before the event. Though less pronounced, the increase in eBC concentration was also seen at 50 m and 4 m, with 130% (1.48 $\mu g/m^3$) and 56% (1.66 $\mu g/m^3$) increase, respectively. The observed increase in eBC concentration at 100 m, just at the PBL height, suggests that while ground-level emission had some impact, local atmospheric conditions allowed for some degree of vertical transport of eBC from the above layer, likely influenced by long-distance transported particles. This is supported by the back trajectory analyses, showing a change in trajectories from south to west at the beginning of the event, associated with fast transport of continental air masses from both longer distances and higher altitudes, with the upper levels (arriving at 500 m) changing first (Figure S13). The drone measurements not only support the

https://doi.org/10.5194/egusphere-2025-1420
Preprint. Discussion started: 16 April 2025

measurements at the building (Figure S10), showing higher $PM_{2.5}$ and PM_{10} concentrations at 50 m compared to 10 m results, but also provide measurements at 100 m, confirming the largest enhancement in eBC concentration during the event above the building compared to the ground and 50 m.

In contrast, PNC showed the highest increase at 4 m and 50 m in comparison to the day before the pollution event, where PNC increased by 840 % (238 particles/cm^3) and 860 % (151 #/cm^3), respectively, with a less pronounced increase at 100 m (460 %, 137 #/cm^3). This suggests that some particles, most likely generated from ground sources, remained concentrated near the surface due to the limited vertical dispersion during the pollution episode. Prior to the event, eBC concentrations exhibited a significant decrease (by 73 %) from the ground up to 100 m, and PNC decreased by 38 % between 4 m and 50 m. However, the trend was notably altered during the event, with no significant change in both eBC and PNC with the height.

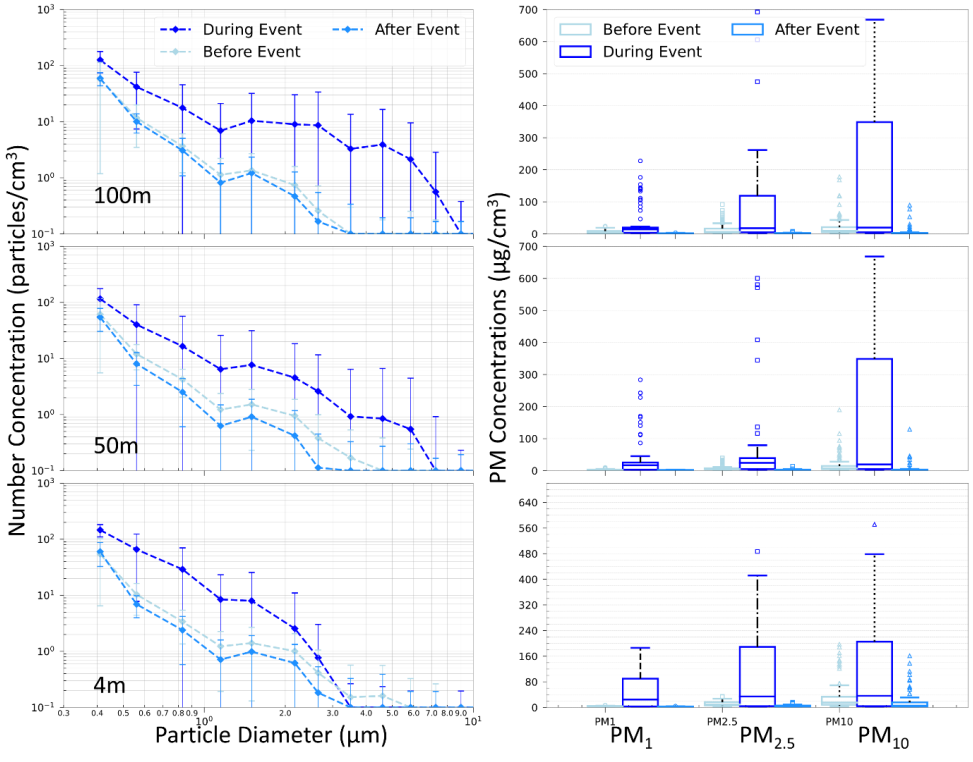

Figure 9. Mean particle number concentration dependence on particle size from OPC on the drone at different heights before, during, and after the high pollution event in Prague.

The particle number size distributions at various heights reveal additional information (Figure 9). At 4m, the concentration of particles smaller than 3 µm increased significantly during the event compared to the distribution before the event, highlighting the production and accumulation of small particles near the ground. In contrast, at 50 m and 100 m, concentrations of all particles were increased during the event, up to sizes of 10 µm. With the height, mainly the concentration of intermodal fraction, i.e., in sizes between 2.5 and 10 µm, increased in concentrations, potentially indicating contribution from longer distance transported aerosol and mixing

https://doi.org/10.5194/egusphere-2025-1420
Preprint. Discussion started: 16 April 2025

processes that redistribute particles vertically. Before the event, particles up to 4 µm in diameter were observed near the ground due to winter stable atmospheric conditions (Gani et al., 2019), which restricted vertical mixing and limited dispersion of pollutants. During the event, a substantial increase in larger particles was observed at 100 m (and partly also at 50 m), while almost no change was observed at the ground level concentrations, remaining below 0.1 #/cm^3, suggesting contributions from long-range transport disconnected from the ground. A significant increase in PM mass was also observed across all heights (4 m, 50 m, and 100 m) (Figure S14). PM_1 and $PM_{2.5}$ dominated the mass concentrations across all heights during the event, while PM_{10} saw the largest increase at 100 m, again suggesting contributions from coarse particles and vertical mixing.

3.5. Seasonal Contrast

The vertical profiles of eBC mass concentration and PNCs in summer and winter were compared, revealing significant differences in the seasonal vertical patterns between the two stations.

At NAOK in winter, a 100% (0.45 µg/m^3) higher eBC mass concentration up to 50 m was found compared to summer (Figure 10a). This difference can be attributed to more stable atmospheric conditions (isothermic to temperature inversion) hindering vertical mixing and to an increased number of sources during winter. At 100 m, the difference between winter and summer eBC mass concentration surged to 200% (0.5 µg/m^3), as in summer, a decrease in eBC concentrations was observed above 50 m, while it was observed from 100 m in winter. In contrast, during the winter campaign at Prague, eBC mass concertation was 80% (0.88 µg/m^3) higher at the ground level compared to summer, but the difference decreased to 24 % (0.32 µg/m^3) at 50 m (Figure 10b). No significant difference in eBC mass concentrations in summer and winter was found at 100 m, indicating effective dispersion at this altitude at Prague, likely influenced by local factors such as the surrounding plateau, which alters airflow patterns and enhances the mixing of pollutants above the top of the valley.

For PNC at NAOK, a 200% (19 #/cm^3) increase was observed at ground level during winter compared to summer, which extended to 336 % (26 #/cm^3) at 50 m and 200 % (148 #/cm^3) at 100m (Figure 10c). However, at 150 m, the difference dropped to 10% (1 #/cm^3), suggesting that particles disperse horizontally more rapidly than vertically at this altitude, likely due to atmospheric stability restricting vertical movements during winter. This is further supported by wind shear values between 100 – 150 m, which were 1.6 m/s per 100 m during summer, indicating higher turbulence and stronger vertical mixing. In contrast, winter exhibited lower wind shear (0.5 m/s per 100 m), signaling reduced turbulence and weaker vertical mixing (Figure S9), favoring horizontal dispersion over vertical transport.

In contrast, in Prague, the PNC behaved differently i.e., higher concentration was measured in summer compared to winter. The particle concentrations decreased with the height more during winter compared to summer (Figure 10d), with only a small difference at the ground level (15 %) (7 #/cm^3) and a higher difference at 50 m and 100 m (36 %, i.e. 10 #/cm^3 and 34 %, i.e. 12 #/cm^3 respectively).

https://doi.org/10.5194/egusphere-2025-1420
Preprint. Discussion started: 16 April 2025

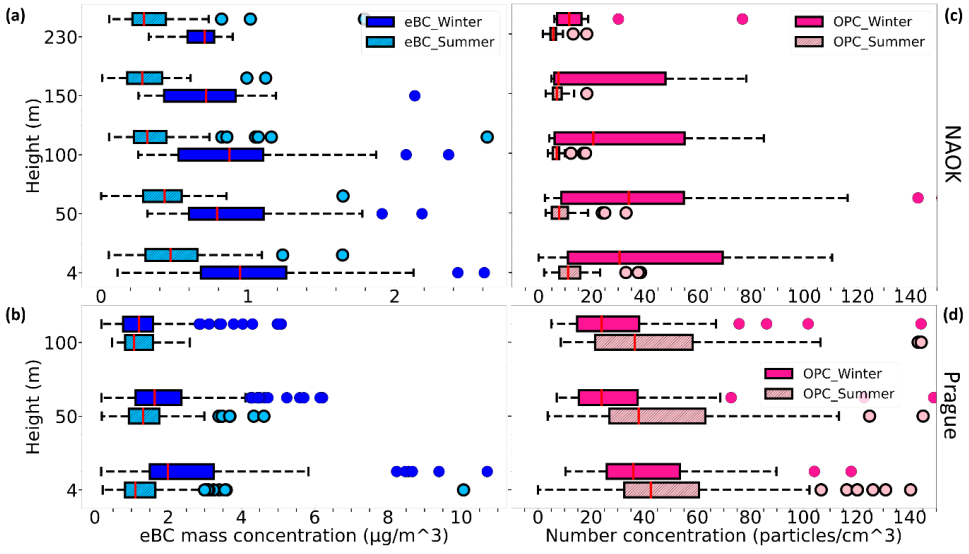

Figure 10. Boxplots of eBC mass concentration from AE51 and PNC from OPC on the drone during summer and winter at (a, c) NAOK and (b, d) Prague.

To understand these patterns further, particle size distribution was examined for the summer and winter campaigns at NAOK and Prague (Figure 11). It is important to note that the size distribution analysis excluded the high pollution event for Prague to avoid skewed results. At the NAOK site, the observed increase in PNC during winter compared to summer was primarily due to increased PM_1 (particles less than or equal to 1 µm in size) across all the heights. Both seasons showed a general decline in concentration as particle size increased; however, winter concentrations were consistently higher across all sizes (up to 3 µm). This suggests that the increase in PNC during winter at NAOK is primarily due to fine-mode particles, often associated with combustion sources like residential heating (Hand et al., 2012). In contrast, summer exhibits lower concentrations and smaller particle sizes, likely due to enhanced vertical mixing and reduced emission sources.

https://doi.org/10.5194/egusphere-2025-1420
Preprint. Discussion started: 16 April 2025

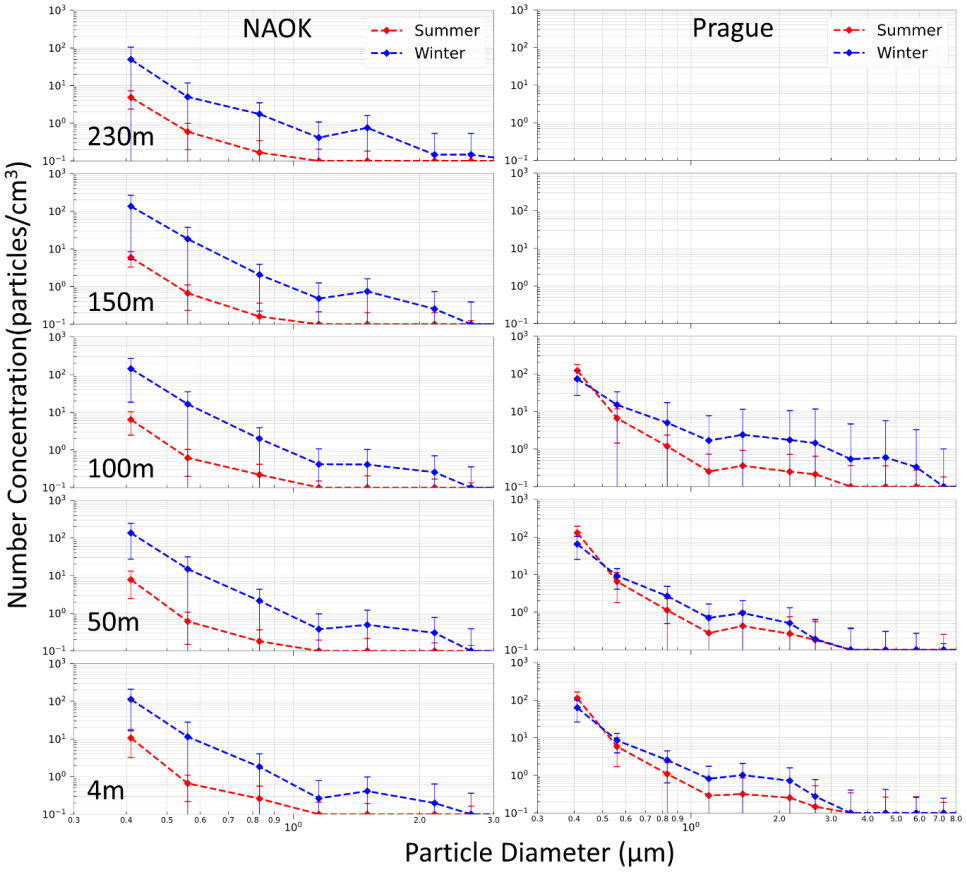

Figure 11. Log-Log plot of the variation of mean particle number concentration with particle size from OPC on the drone at different heights during summer (red) and winter (blue) at NAOK (left) and Prague (right).

At the urban site, Prague, the size distribution analysis showed a significant increase in the average particle count for particles with sizes between 0.5 – 3 µm during winter compared to summer across all heights. Despite this increase, PNC was higher in summer than in winter (Figure 10d) due to higher summer concentrations in the smallest size bin, < 0.5 µm (Figure 11). Although not fully recorded by OPC due to its size limit, these particles could be attributed to new particle formation from photochemical reactions. This is supported by the higher concentration of nitrogen dioxide (NO_2) during summer (Figure S15), combined with increased sunlight (Figure S16). Indeed, regions with higher NO_x levels, such as urban areas, tend to have more frequent and intense new particle formation events (Gao et al., 2012; Kulmala et al., 2004). The larger particles (2.5 - 8 µm) showed a more significant increase during winter in Prague, particularly at 100m, further suggesting contributions from regional or long-range transported sources.

https://doi.org/10.5194/egusphere-2025-1420
Preprint. Discussion started: 16 April 2025

4. Summary and conclusions

This study presents a comprehensive analysis of vertical measurements of eBC mass concentration and PNC using drone-based profiling at a rural (NAOK) and an urban (Prague) site in the Czech Republic during different seasons. A comparison of drone-deployed instruments with reference measurements at various heights of fixed observational platforms (tall tower and building) was performed under various RH conditions and RH control strategies.

The results show the effectiveness of drones for vertical profiling, offering results comparable to reference instruments at various heights between 0 and 230 m and suggesting the applicability of drone eBC and PNC measurements also in higher altitudes. When mounted on a drone, eBC mass concentrations from AE51 with dryer were comparable at the ground and 230 m with the reference devices. Without the dryer, the eBC mass concentration was overestimated by 276 % and 285% compared to the reference devices on the ground during summer and winter, respectively, attributed to higher ambient RH levels. In comparison, results differ by less than 10 % from the reference when using a dryer. Thus, drying significantly reduces measurement discrepancies, highlighting the importance of drying in minimizing the impact of RH, particularly for eBC measurements. These findings emphasize the necessity of a drying system even on drone-based measurement platforms.

At the rural site (NAOK), eBC mass concentration and PNC decreased with height during both seasons, though the height at which the decrease began was higher in winter than in summer. eBC mass concentrations were uniformly distributed up to the first 50 m in summer and up to 100 m in winter. PNC decreased with the height from the ground in summer, while it stayed uniform up to 50 m in winter, probably due to the stable atmospheric conditions during this season, which also led to higher concentrations for both eBC and PNC compared to summer. The higher concentrations during winter at NAOK were primarily driven by fine particles (PM_1) associated with combustion sources such as residential heating. However, our results suggest that at least two aerosol populations of different sizes and sources were measured during the year, thus with different vertical behaviors.

Conversely, at the urban site (Prague), both eBC and PNC were more uniform across altitudes in summer, facilitated by strong emission sources and enhanced vertical mixing driven by the urban heat island effect. eBC mass concentration and PNC in winter decrease with height, reflecting limited vertical mixing due to more stable atmospheric conditions. PNC was higher in summer, likely due to increased secondary particle formation driven by elevated levels of gaseous precursors and photochemical reactions. During a winter high pollution event in Prague, both eBC and PNC concentrations increased, with long-range transport contributing to high eBC mass at 100m, while PNC remained concentrated near the surface. These emphasize the dynamic interaction of local emissions, atmospheric stability, and long-range transport aerosols in shaping vertical concentration profiles, undecipherable by only ground-based measurements. Using drone-based measurements to capture vertical variation in air quality offers valuable insights into pollutant dynamics.

Author contribution

KJ, DB, and NZ designed the experiments. KJ carried out all the experiments. KJ was also responsible for conceptualization, methodology, validation, formal analysis, investigation, data curation, visualization, and writing of the original draft. DB contributed to methodology and writing – review & editing. NZ was responsible

https://doi.org/10.5194/egusphere-2025-1420
Preprint. Discussion started: 16 April 2025

for validation, supervision, and writing – review & editing. SM was responsible for data curation and contributed to writing – review & editing. VZ contributed to writing – review & editing, funding acquisition, and resources.

Data availability

The dataset including drone measured data and from reference devices and meteorological instruments, covering both rural and urban sites across different seasons is available at JULAHA, KAJAL (2025), "Drone_rural_urban", Mendeley Data, V1, doi: 10.17632/snbp6w49v9.1

Acknowledgment

We gratefully acknowledge the financial support provided by the National Research Infrastructure Support Project - ACTRIS Participation of the Czech Republic (ACTRIS-CZ LM2023030) and CzeCOS (LM2023048), funded by the Ministry of Education, Youth and Sports of the Czech Republic, and the Czech Science Foundation under grant 24-10768S, ICPF Internal Grant Agency (IGA - 028001) and Charles University Grant Agency (grant number 98124). We also thank colleagues from the Košetice observatory and Department of Atmospheric Physics, Prague, for providing the meteorological data. Special Thanks to our technicians, Petr Roztočil and Rohit, for preparing the Arduino datalogger and Airstream Dryer.

References

Alas, H. D. C., Müller, T., Weinhold, K., Pfeifer, S., Glojek, K., Gregorič, A., Močnik, G., Drinovec, L., Costabile, F., Ristorini, M., and Wiedensohler, A.: Performance of microAethalometers: Real-world Field Intercomparisons from Multiple Mobile Measurement Campaigns in Different Atmospheric Environments, Aerosol Air Qual. Res., 20, 2640–2653, https://doi.org/10.4209/aaqr.2020.03.0113, 2020.

Altstädter, B., Deetz, K., Vogel, B., Babić, K., Dione, C., Pacifico, F., Jambert, C., Ebus, F., Bärfuss, K., and Pätzold, F.: The vertical variability of black carbon observed in the atmospheric boundary layer during DACCIWA, Atmospheric chemistry and physics, 20, 7911–7928, 2020.

Metrostav: https://www.metrostav.cz/en/segments/tunnelling/references/28-blanka-tunnel-complex, last access: 11 December 2024.

Babu, S. S., Moorthy, K. K., Manchanda, R. K., Sinha, P. R., Satheesh, S. K., Vajja, D. P., Srinivasan, S., and Kumar, V. H. A.: Free tropospheric black carbon aerosol measurements using high altitude balloon: Do BC layers build "their own homes" up in the atmosphere?: FREE TROPOSPHERIC BLACK CARBON AEROSOL, Geophys. Res. Lett., 38, n/a-n/a, https://doi.org/10.1029/2011GL046654, 2011.

Barbieri, L., Kral, S. T., Bailey, S. C. C., Frazier, A. E., Jacob, J. D., Reuder, J., Brus, D., Chilson, P. B., Crick, C., Detweiler, C., Doddi, A., Elston, J., Foroutan, H., González-Rocha, J., Greene, B. R., Guzman, M. I., Houston, A. L., Islam, A., Kemppinen, O., Lawrence, D., Pillar-Little, E. A., Ross, S. D., Sama, M. P., Schmale, D. G., Schuyler, T. J., Shankar, A., Smith, S. W., Waugh, S., Dixon, C., Borenstein, S., and de Boer, G.: Intercomparison of Small Unmanned Aircraft System (sUAS) Measurements for Atmospheric Science during the LAPSE-RATE Campaign, Sensors, 19, 2179, https://doi.org/10.3390/s19092179, 2019.

Battaglia, M. A., Douglas, S., and Hennigan, C. J.: Effect of the Urban Heat Island on Aerosol pH, Environ. Sci. Technol., 51, 13095–13103, https://doi.org/10.1021/acs.est.7b02786, 2017.

Boer, G. de, Diehl, C., Jacob, J., Houston, A., Smith, S. W., Chilson, P., Schmale, D. G., Intrieri, J., Pinto, J., Elston, J., Brus, D., Kemppinen, O., Clark, A., Lawrence, D., Bailey, S. C. C., Sama, M. P., Frazier, A., Crick, C., Natalie, V., Pillar-Little, E., Klein, P., Waugh, S., Lundquist, J. K., Barbieri, L., Kral, S. T., Jensen, A. A., Dixon, C., Borenstein, S., Hesselius, D., Human, K., Hall, P., Argrow, B., Thornberry, T., Wright, R., and Kelly, J. T.: Development of Community, Capabilities, and Understanding through Unmanned Aircraft-Based Atmospheric Research: The LAPSE-RATE Campaign, https://doi.org/10.1175/BAMS-D-19-0050.1, 2020.

https://doi.org/10.5194/egusphere-2025-1420
Preprint. Discussion started: 16 April 2025

Bond, T. C., Doherty, S. J., Fahey, D. W., Forster, P. M., Berntsen, T., DeAngelo, B. J., Flanner, M. G., Ghan, S., Kärcher, B., Koch, D., Kinne, S., Kondo, Y., Quinn, P. K., Sarofim, M. C., Schultz, M. G., Schulz, M., Venkataraman, C., Zhang, H., Zhang, S., Bellouin, N., Guttikunda, S. K., Hopke, P. K., Jacobson, M. Z., Kaiser, J. W., Klimont, Z., Lohmann, U., Schwarz, J. P., Shindell, D., Storelvmo, T., Warren, S. G., and Zender, C. S.: Bounding the role of black carbon in the climate system: A scientific assessment, JGR Atmospheres, 118, 5380–5552, https://doi.org/10.1002/jgrd.50171, 2013.

Brady, J. M., Stokes, M. D., Bonnardel, J., and Bertram, T. H.: Characterization of a Quadrotor Unmanned Aircraft System for Aerosol-Particle-Concentration Measurements, Environ. Sci. Technol., 50, 1376–1383, https://doi.org/10.1021/acs.est.5b05320, 2016.

Brus, D., Gustafsson, J., Vakkari, V., Kemppinen, O., de Boer, G., and Hirsikko, A.: Measurement report: Properties of aerosol and gases in the vertical profile during the LAPSE-RATE campaign, Atmospheric Chemistry and Physics, 21, 517–533, https://doi.org/10.5194/acp-21-517-2021, 2021.

Brus, D., Le, V., Kuula, J., and Doulgeris, K.: Data collected by a drone backpack for air quality and atmospheric state measurements during Pallas Cloud Experiment 2022 (PaCE2022), Earth System Science Data Discussions, 1–14, https://doi.org/10.5194/essd-2025-61, 2025.

Cappelletti, D., Petroselli, C., Mateos, D., Herreras, M., Ferrero, L., Losi, N., Gregorič, A., Frangipani, C., La Porta, G., and Lonardi, M.: Vertical profiles of black carbon and nanoparticles pollutants measured by a tethered balloon in Longyearbyen (Svalbard islands), Atmospheric Environment, 290, 119373, 2022.

Chen, D., Liao, H., Yang, Y., Chen, L., Zhao, D., and Ding, D.: Simulated impacts of vertical distributions of black carbon aerosol on meteorology and PM 2.5 concentrations in Beijing during severe haze events, Atmospheric Chemistry and Physics, 22, 1825–1844, 2022.

Chi, X., Winderlich, J., Mayer, J.-C., Panov, A. V., Heimann, M., Birmili, W., Heintzenberg, J., Cheng, Y., and Andreae, M. O.: Long-term measurements of aerosol and carbon monoxide at the ZOTTO tall tower to characterize polluted and pristine air in the Siberian taiga, Atmospheric Chemistry and Physics, 13, 12271–12298, 2013.

Chilinski, M. T., Markowicz, K. M., and Markowicz, J.: Observation of vertical variability of black carbon concentration in lower troposphere on campaigns in Poland, Atmospheric Environment, 137, 155–170, https://doi.org/10.1016/j.atmosenv.2016.04.020, 2016.

Corrigan, C. E., Roberts, G. C., Ramana, M. V., Kim, D., and Ramanathan, V.: Capturing vertical profiles of aerosols and black carbon over the Indian Ocean using autonomous unmanned aerial vehicles, Atmospheric Chemistry and Physics Discussions, 7, 11429–11463, 2007.

CSD: https://www.rsd.cz/silnice-a-dalnice/scitani-dopravy, last access: 11 December 2024.

Ding, A. J., Huang, X., Nie, W., Sun, J. N., Kerminen, V. -M., Petäjä, T., Su, H., Cheng, Y. F., Yang, X. -Q., Wang, M. H., Chi, X. G., Wang, J. P., Virkkula, A., Guo, W. D., Yuan, J., Wang, S. Y., Zhang, R. J., Wu, Y. F., Song, Y., Zhu, T., Zilitinkevich, S., Kulmala, M., and Fu, C. B.: Enhanced haze pollution by black carbon in megacities in China, Geophysical Research Letters, 43, 2873–2879, https://doi.org/10.1002/2016GL067745, 2016.

Dvorská, A., Sedlák, P., Schwarz, J., Fusek, M., Hanuš, V., Vodička, P., and Trusina, J.: Atmospheric station Křešín u Pacova, Czech Republic–a Central European research infrastructure for studying greenhouse gases, aerosols and air quality, Advances in Science and Research, 12, 79–83, 2015.

Ferrero, L., Ritter, C., Cappelletti, D., Moroni, B., Močnik, G., Mazzola, M., Lupi, A., Becagli, S., Traversi, R., and Cataldi, M.: Aerosol optical properties in the Arctic: The role of aerosol chemistry and dust composition in a closure experiment between Lidar and tethered balloon vertical profiles, Science of the total environment, 686, 452–467, 2019.

Gani, S., Bhandari, S., Seraj, S., Wang, D. S., Patel, K., Soni, P., Arub, Z., Habib, G., Hildebrandt Ruiz, L., and Apte, J. S.: Submicron aerosol composition in the world's most polluted megacity: the Delhi Aerosol Supersite study, Atmospheric Chemistry and Physics, 19, 6843–6859, 2019.

https://doi.org/10.5194/egusphere-2025-1420
Preprint. Discussion started: 16 April 2025

Gao, J., Chai, F., Wang, T., Wang, S., and Wang, W.: Particle number size distribution and new particle formation: New characteristics during the special pollution control period in Beijing, Journal of Environmental Sciences, 24, 14–21, https://doi.org/10.1016/S1001-0742(11)60725-0, 2012.

Haeffelin, M., Ribaud, J.-F., Kotthaus, S., Dupont, J.-C., Lemonsu, A., and Masson, V.: Effect of nocturnal urban boundary layer stability and mixing on temperature contrasts between built-up environments and urban parks, Copernicus Meetings, https://doi.org/10.5194/egusphere-egu24-19030, 2024.

Hagan, D. H. and Kroll, J. H.: Assessing the accuracy of low-cost optical particle sensors using a physics-based approach, Atmospheric Measurement Techniques, 13, 6343–6355, https://doi.org/10.5194/amt-13-6343-2020, 2020.

Hand, J. L., Schichtel, B. A., Pitchford, M., Malm, W. C., and Frank, N. H.: Seasonal composition of remote and urban fine particulate matter in the United States, Journal of Geophysical Research: Atmospheres, 117, https://doi.org/10.1029/2011JD017122, 2012.

Harm-Altstädter, B., Voß, A., Aust, S., Bärfuss, K., Bretschneider, L., Merkel, M., Pätzold, F., Schlerf, A., Weinhold, K., Wiedensohler, A., Winkler, U., and Lampert, A.: First study using a fixed-wing drone for systematic measurements of aerosol vertical distribution close to a civil airport, Frontiers in Environmental Science, 12, https://doi.org/10.3389/fenvs.2024.1376980, 2024.

Hersbach, H., Bell, B., Berrisford, P., Biavati, G., Horányi, A., Muñoz Sabater, J., Nicolas, J., Peubey, C., Radu, R., and Rozum, I.: ERA5 hourly data on single levels from 1979 to present, Copernicus climate change service (c3s) climate data store (cds), 10, 2018.

Julaha, K., Ždímal, V., Holubová Šmejkalová, A., Komínková, K., and Zíková, N.: Boundary layer and mixing layer height: Models vs. Ground-based measurements intercomparison, Atmospheric Research, 315, 107897, https://doi.org/10.1016/j.atmosres.2024.107897, 2025.

Kotthaus, S., Haeffelin, M., Céspedes, J., Van Hove, M., Drouin, M.-A., Dupont, J.-C., and Foret, G.: Urban atmosphere dynamics for air quality applications: Atmospheric boundary layer height and wind profiles from ground-based remote sensing networks, EGU-13154, https://doi.org/10.5194/egusphere-egu23-13154, 2023.

Kulmala, M., Vehkamäki, H., Petäjä, T., Dal Maso, M., Lauri, A., Kerminen, V.-M., Birmili, W., and McMurry, P. H.: Formation and growth rates of ultrafine atmospheric particles: a review of observations, Journal of Aerosol Science, 35, 143–176, https://doi.org/10.1016/j.jaerosci.2003.10.003, 2004.

Li, J., Von Salzen, K., Peng, Y., Zhang, H., and Liang, X.: Evaluation of black carbon semi–direct radiative effect in a climate model, JGR Atmospheres, 118, 4715–4728, https://doi.org/10.1002/jgrd.50327, 2013.

Liang, Y., Wu, C., Wu, D., Liu, B., Li, Y. J., Sun, J., Yang, H., Mao, X., Tan, J., and Xia, R.: Vertical distributions of atmospheric black carbon in dry and wet seasons observed at a 356-m meteorological tower in Shenzhen, South China, Science of the Total Environment, 853, 158657, 2022.

Liu, B., Wu, C., Ma, N., Chen, Q., Li, Y., Ye, J., Martin, S. T., and Li, Y. J.: Vertical profiling of fine particulate matter and black carbon by using unmanned aerial vehicle in Macau, China, Science of The Total Environment, 709, 136109, https://doi.org/10.1016/j.scitotenv.2019.136109, 2020.

Liu, H., Pan, X., Lei, S., Zhang, Y., Du, A., Yao, W., Tang, G., Wang, T., Xin, J., and Li, J.: Vertical distribution of black carbon and its mixing state in the urban boundary layer in summer, Atmospheric Chemistry and Physics, 23, 7225–7239, 2023.

Lumet, E., Jaravel, T., Rochoux, M. C., Vermorel, O., and Lacroix, S.: Assessing the Internal Variability of Large-Eddy Simulations for Microscale Pollutant Dispersion Prediction in an Idealized Urban Environment, Boundary-Layer Meteorol, 190, 9, https://doi.org/10.1007/s10546-023-00853-7, 2024.

Mbengue, S., Zikova, N., Schwarz, J., Vodička, P., Šmejkalová, A. H., and Holoubek, I.: Mass absorption cross-section and absorption enhancement from long term black and elemental carbon measurements: A rural background station in Central Europe, Science of The Total Environment, 794, 148365, https://doi.org/10.1016/j.scitotenv.2021.148365, 2021.

https://doi.org/10.5194/egusphere-2025-1420
Preprint. Discussion started: 16 April 2025

Mbengue, S., Vodička, P., Komínková, K., Zíková, N., Schwarz, J., Prokeš, R., Suchánková, L., Julaha, K., Ondráček, J., and Holoubek, I.: Different approaches to explore the impact of COVID-19 lockdowns on carbonaceous aerosols at a European rural background site, Science of the Total Environment, 892, 164527, 2023.

Mizera, J., Havelcová, M., Machovič, V., Borecká, L., and Vöröš, D.: Neutron Activation Analysis in Urban Geochemistry: Impact of Traffic Intensification after Opening the Blanka Tunnel Complex in Prague, Minerals, 12, 281, https://doi.org/10.3390/min12030281, 2022.

Moteki, N.: Climate-relevant properties of black carbon aerosols revealed by in situ measurements: a review, Prog Earth Planet Sci, 10, 12, https://doi.org/10.1186/s40645-023-00544-4, 2023.

Myhre, G., Myhre, C. E. L., Samset, B. H., and Storelvmo, T.: Aerosols and their relation to global climate and climate sensitivity, Nature Education Knowledge, 4, 7, 2013.

Petzold, A., Schloesser, H., Sheridan, P., Arnott, W., Ogren, J., and Virkkula, A.: Evaluation of Multiangle Absorption Photometry for Measuring Aerosol Light Absorption, Aerosol Science and Technology, 39, 40–51, https://doi.org/10.1080/027868290901945, 2005.

Ramana, M. V., Ramanathan, V., Feng, Y., Yoon, S. C., Kim, S. W., Carmichael, G. R., and Schauer, J. J.: Warming influenced by the ratio of black carbon to sulphate and the black-carbon source, Nature Geoscience, 3, 542–545, 2010.

Ramanathan, V. and Carmichael, G.: Global and regional climate changes due to black carbon, Nature geoscience, 1, 221–227, 2008.

Ramatheerthan, S. K., Peiker, J., Crespo, N. M., and Kozubek, M.: Monitoring Extreme Meteorological and Pollution Events in Prague: A Station Data Based Analysis, WDS'24 Proceedings of Contributed Papers — Physics (eds. J. Šafránková and J. Pavlů), 9–18, 2024.

Renard, J.-B., Michoud, V., and Giacomoni, J.: Vertical profiles of pollution particle concentrations in the boundary layer above Paris (France) from the optical aerosol counter LOAC onboard a touristic balloon, Sensors, 20, 1111, 2020.

Samad, A., Vogt, U., Panta, A., and Uprety, D.: Vertical distribution of particulate matter, black carbon and ultra-fine particles in Stuttgart, Germany, Atmospheric Pollution Research, 11, 1441–1450, https://doi.org/10.1016/j.apr.2020.05.017, 2020.

Samset, B. H., Myhre, G., Schulz, M., Balkanski, Y., Bauer, S., Berntsen, T. K., Bian, H., Bellouin, N., Diehl, T., and Easter, R. C.: Black carbon vertical profiles strongly affect its radiative forcing uncertainty, Atmospheric Chemistry and Physics, 13, 2423–2434, 2013.

Schulz, H., Zanatta, M., Bozem, H., Leaitch, W. R., Herber, A. B., Burkart, J., Willis, M. D., Kunkel, D., Hoor, P. M., and Abbatt, J. P.: High Arctic aircraft measurements characterising black carbon vertical variability in spring and summer, Atmospheric Chemistry and Physics, 19, 2361–2384, 2019.

Schwarz, J. P., Gao, R. S., Fahey, D. W., Thomson, D. S., Watts, L. A., Wilson, J. C., Reeves, J. M., Darbeheshti, M., Baumgardner, D. G., Kok, G. L., Chung, S. H., Schulz, M., Hendricks, J., Lauer, A., Kärcher, B., Slowik, J. G., Rosenlof, K. H., Thompson, T. L., Langford, A. O., Loewenstein, M., and Aikin, K. C.: Single-particle measurements of midlatitude black carbon and light-scattering aerosols from the boundary layer to the lower stratosphere, J. Geophys. Res., 111, 2006JD007076, https://doi.org/10.1029/2006JD007076, 2006.

Sun, T., Wu, C., Wu, D., Liu, B., Sun, J. Y., Mao, X., Yang, H., Deng, T., Song, L., Li, M., Li, Y. J., and Zhou, Z.: Time-resolved black carbon aerosol vertical distribution measurements using a 356-m meteorological tower in Shenzhen, Theor Appl Climatol, 140, 1263–1276, https://doi.org/10.1007/s00704-020-03168-6, 2020.

Villa, T. F., Salimi, F., Morton, K., Morawska, L., and Gonzalez, F.: Development and validation of a UAV based system for air pollution measurements, Sensors, 16, 2202, 2016.

https://doi.org/10.5194/egusphere-2025-1420
Preprint. Discussion started: 16 April 2025

Vodička, P., Schwarz, J., Cusack, M., and Ždímal, V.: Detailed comparison of OC/EC aerosol at an urban and a rural Czech background site during summer and winter, Science of The Total Environment, 518–519, 424–433, https://doi.org/10.1016/j.scitotenv.2015.03.029, 2015.

Wang, Q., Sun, Y., Xu, W., Du, W., Zhou, L., Tang, G., Chen, C., Cheng, X., Zhao, X., Ji, D., Han, T., Wang, Z., Li, J., and Wang, Z.: Vertically resolved characteristics of air pollution during two severe winter haze episodes in urban Beijing, China, Atmospheric Chemistry and Physics, 18, 2495–2509, https://doi.org/10.5194/acp-18-2495-2018, 2018a.

Wang, Y., Vogel, J. M., Lin, Y., Pan, B., Hu, J., Liu, Y., Dong, X., Jiang, J. H., Yung, Y. L., and Zhang, R.: Aerosol microphysical and radiative effects on continental cloud ensembles, Advances in Atmospheric Sciences, 35, 234–247, 2018b.

von der Weiden, S.-L., Drewnick, F., and Borrmann, S.: Particle Loss Calculator – a new software tool for the assessment of the performance of aerosol inlet systems, Atmospheric Measurement Techniques, 2, 479–494, https://doi.org/10.5194/amt-2-479-2009, 2009.

Wu, C., Liu, B., Wu, D., Yang, H., Mao, X., Tan, J., Liang, Y., Sun, J. Y., Xia, R., and Sun, J.: Vertical profiling of black carbon and ozone using a multicopter unmanned aerial vehicle (UAV) in urban Shenzhen of South China, Science of the Total Environment, 801, 149689, 2021.

Xie, C., Xu, W., Wang, J., Wang, Q., Liu, D., Tang, G., Chen, P., Du, W., Zhao, J., and Zhang, Y.: Vertical characterization of aerosol optical properties and brown carbon in winter in urban Beijing, China, Atmospheric Chemistry and Physics, 19, 165–179, 2019.

Zhu, Y., Wu, Z., Park, Y., Fan, X., Bai, D., Zong, P., Qin, B., Cai, X., and Ahn, K.-H.: Measurements of atmospheric aerosol vertical distribution above North China Plain using hexacopter, Science of The Total Environment, 665, 1095–1102, https://doi.org/10.1016/j.scitotenv.2019.02.100, 2019.